Noname manuscript No.
(will be inserted by the editor)

SPACE: the SPectroscopic All-sky Cosmic Explorer

A. Cimatti · M. Robberto · C. Baugh ·
S. V. W. Beckwith · R. Content · E.
Daddi · G. De Lucia · B. Garilli · L.
Guzzo · G. Kauffmann · M. Lehnert ·
D. Maccagni · A. Martinez-Sansigre ·
F. Pasian · I. N. Reid · P. Rosati · R.
Salvaterra · M. Stiavelli · Y. Wang ·
M. Zapatero Osorio · M. Balcells · M.
Bersanelli · F. Bertoldi · J. Blaizot ·
D. Bottini · R. Bower · A. Bulgarelli ·
A. Burgasser · C. Burigana · R. C.
Butler · S. Casertano · B. Ciardi · M.
Cirasuolo · M. Clampin · S. Cole ·
A. Comastri · S. Cristiani · J.-G.
Cuby · F. Cuttaia · A. De Rosa ·
A. Diaz Sanchez · M. Di Capua · J.
Dunlop · X. Fan · A. Ferrara · F.
Finelli · A. Franceschini · M. Franx · P.
Franzetti · C. Frenk · J. Gardner · F.
Gianotti · R. Grange · C. Gruppioni ·
A. Gruppuso · F. Hammer · L.
Hillenbrand · A. Jacobesn · M. Jarvis ·
R. Kennicutt · R. Kimble · M. Kriek ·
J. Kurk · J.-P. Kneib · O. Le Fevre · D.
Macchetto · J. MacKenty · P. Madau ·
M. Magliocchetti · N. Mandolesi · R.
McLure · M. Meyer · M. Mignoli · · B.
Mobasher · E. Molinari · G. Morgante ·
S. Morris · L. Nicastro · T. Oliva · P.
Padovani · E. Palazzi · F. Paresce · A.
Perez Garrido · E. Pian · L. Popa · M.
Postman · L. Pozzetti · J. Rayner · R.
Rebolo · A. Renzini · H. Röttgering ·
E. Schinnerer · M. Scodeggio · M.
Saisse · T. Shanks · A. Shapley · R.
Sharples · H. Shea · J. Silk · I. Smail ·
P. Spanó · J. Steinacker · M. Strauss ·
L. Stringhetti · A. Szalay · L. Tresse ·
M. Trifoglio · M. Urry · L. Valenziano ·
F. Villa · I. Villo Perez · F. Walter ·

M. Ward · R. White · S. White · N. Wright · R. Wyse · G. Zamorani · A. Zacchei · W. Zeilinger · F. Zerbi

A. Cimatti (Principal Investigator)
Università di Bologna, Dipartimento di Astronomia, Italy E-mail: a.cimatti@unibo.it

M. Robberto (co-Principal Investigator)
Space Telescope Science Institute, Baltimore, USA E-mail: robberto@stsci.edu

C. Baugh (University of Durham, Institute of Computational Cosmology, UK) · S. W. V. Beckwith (STScI, Baltimore, USA) · R. Content (University of Durham, Centre for Advanced Instrumentation, UK) · E. Daddi (CEA Saclay, France) · G. de Lucia (MPA Garching, Germany) · B. Garilli (INAF - IASFMI, Italy) · L. Guzzo (INAF - Brera, Italy) · G. Kauffmann (MPA Garching, Germany) · M. Lehnert (Observatoire de Paris - Meudon, France) · D. Maccagni (INAF - IASFMI, Italy) · A. Martinez-Sansigre (MPIA Heidelberg, Germany) · F. Pasian (INAF - OATS, Italy) · I. N. Reid (STScI, USA) · P. Rosati (ESO Garching, Germany) · R. Salvaterra (University of Milano, Italy) · M. Stiavelli (STScI, USA) · Y. Wang (University of Oklahoma, USA) · M. Zapatero Osorio (IAC, Spain) · M. Balcells (IAC, Spain) · M. Bersanelli (University of Milano, Italy) · F. Bertoldi (University of Bonn, Germany) · J. Blaizot (MPA Garching, Germany) · D. Bottini (INAF - IASFMI, Italy) · R. Bower (University of Durham, UK) · A. Bulgarelli (INAF - IASFBO, Italy) · A. Burgasser (MIT, USA) · C. Burigana (INAF - IASFBO, Italy) · R. C. Butler (INAF - IASFBO, Italy) · S. Casertano (STScI, USA) · B. Ciardi (MPA Garching, Germany) · M. Cirasuolo (ROE, UK) · M. Clampin (GSFC, USA) · S. Cole (University of Durham, UK) · A. Comastri (INAF - OABO, Italy) · S. Cristiani (INAF - OATS, Italy) · J.-G. Cuby (LAM) · F. Cuttaia (INAF - IASFBO, Italy) · A. De Rosa (INAF - IASFBO, Italy) · A. Diaz Sanchez (UPCT, U. Politecnica de Cartagena, Spain) · M. Di Capua (UMD, USA) · J. Dunlop (ROE, UK and CRC, Canada) · X. Fan (University of Arizona, USA) · A. Ferrara (SISSA, Italy) · F. Finelli (INAF - IASFBO, Italy) · A. Franceschini (University of Padova, Italy) · M. Franx (University of Leiden, The Netherlands) · P. Franzetti (INAF - IASFMI, Italy) · C. Frenk (University of Durham, Institute of Computational Cosmology, UK) · J. Gardner (GSFC, USA) · F. Gianotti (INAF - IASFBO, Italy) · R. Grange (LAM, France) · C. Gruppioni (INAF - OABO, Italy) · A. Gruppuso (INAF - IASFBO, Italy) · F. Hammer (Observatoire de Paris - Meudon, France) · L. Hillenbrand (Caltech, USA) · A. Jacobesn (OpSys Project Consulting, Germany) · M. Jarvis (University of Hertfordshire, UK) · R. Kennicutt (IoA, Cambridge, UK) · R. Kimble (GSFC, USA) · M. Kriek (University of Leiden, The Netherlands) · J. Kurk (MPIA Heidelberg, Germany) · J.-P. Kneib (LAM, France) · O. Le Fevre(LAM, France) · D. Macchetto (ESA) · J. MacKenty (STScI, USA) · P. Madau (UCSC, USA) · M. Magliocchetti (INAF - OATS, Italy) · N. Mandolesi (INAF IASFBO, Italy) · R. McLure (ROE, UK) · M. Meyer (Steward Observatory, USA) · M. Mignoli (INAF OABO, Italy) · B. Mobasher (UC Riverside, USA) · E. Molinari (INAF Brera, Italy) · G. Morgante (INAF IASFBO, Italy) · S. Morris (University of Durham, Centre for Advanced Instrumentation, UK) · L. Nicastro (INAF IASFBO, Italy) · T. Oliva (INAF OAA and TNG, Italy) · P. Padovani (ESO Garching, Germany) · E. Palazzi (INAF IASFBO, Italy) · F. Paresce (INAF IASFBO, Italy) · A. Perez Garrido (UPCT, U. Politecnica de Cartagena, Spain) · E. Pian (INAF OATS, Italy) · L. Popa (U. Bucharest, Romania) · M. Postman (STScI, USA) · L. Pozzetti (INAF OABO, Italy) · J. Rayner (Institute for Astronomy, Hawaii, USA) · R. Rebolo (IAC, Spain) · A. Renzini (INAF OAPD, Italy) · H. Roettgering (University of Leiden, The Netherlands) · E. Schinnerer (MPIA Heidelberg, Germany) · M. Scodeggio (INAF IASFMI, Italy) · M. Saisse (LAM, France) · T. Shanks (University of Durham, UK) · A. Shapley (Princeton) · R. Sharples (University of Durham, Centre for Advanced Instrumentation, UK) · H. Shea (Ecole Polytechnique Lausanne, Switzerland) · J. Silk (University of Oxford, UK) · I. Smail (University of Durham, UK) · P. Spanó (INAF Brera, Italy) ·

Abstract We describe the scientific motivations, the mission concept and the instrumentation of *SPACE*, a class-M mission proposed for concept study at the first call of the ESA *Cosmic-Vision 2015-2025* planning cycle. *SPACE* aims at producing the largest three-dimensional evolutionary map of the Universe over the past 10 billion years by taking near-IR spectra and measuring redshifts of more than half a billion galaxies at $0 < z < 2$ down to $AB \sim 23$ over 3π sr of the sky. In addition, *SPACE* will also target a smaller sky field, performing a deep spectroscopic survey of millions of galaxies to $AB \sim 26$ and at $2 < z < 10+$. Owing to the depth, redshift range, volume coverage and quality of its spectra, *SPACE* will reveal with unique sensitivity most of the fundamental cosmological signatures, including the power spectrum of density fluctuations and its turnover, the baryonic acoustic oscillations imprinted when matter and radiation decoupled, the distance-luminosity relation of cosmological supernovae, the evolution of the cosmic expansion rate, the growth rate of cosmic large-scale structure, the large scale distribution of galaxies. The datasets from the *SPACE* mission will represent a long lasting legacy that will be data mined for many years to come.

PACS 98.80.Es Observational cosmology $\cdot$ 95.36.+x Dark energy $\cdot$ 95.55.-n Astronomical and space-research instrumentation

1 Introduction

Our view of the Universe has changed dramatically over the past two decades through measurements of the cosmic microwave background, the large-scale structure of the local Universe ($z < 0.3$) and the brightness of distant supernovae. Fully 96% of the constituents consist of non-luminous and unidentified dark energy (73%) and dark matter (23%) that govern the expansion history and evolution of cosmic structure and leave their imprints on the structure and distribution of visible galaxies. These dark components are unexplained in standard physical theory. The resolution to this mystery through new particles or modification to the theories of gravity, quantum mechanics or the standard model, is considered the most important problem in physics. These unidentified dark components are, nevertheless, considered a natural feature of standard cosmology because they can explain a wide range of observations assuming only that dark energy produces a pressure countering gravity and dark matter behaves like ordinary matter in its effect on space-time. A standard picture has emerged in which cosmological structures develop through

J. Steinacker (MPIA Heidelberg, Germany) $\cdot$ M. Strauss (Princeton, USA) $\cdot$ L. Stringhetti (INAF IASFBO, Italy) $\cdot$ A. Szalay (Johns Hopkins University, USA) $\cdot$ L. Tresse (LAM, France) $\cdot$ M. Trifoglio (INAF IASFBO, Italy) $\cdot$ M. Urry (Yale, USA) $\cdot$ L. Valenziano (INAF IASFBO, Italy) $\cdot$ F. Villa (INAF IASFBO, Italy) $\cdot$ I. Villo Perez (UPCT, U. Politecnica de Cartagena, Spain) $\cdot$ F. Walter (MPIA Heidelberg, Germany) $\cdot$ M. Ward (University of Durham, UK) $\cdot$ R. White (STScI, USA) $\cdot$ S. White (MPA Garching, Germany) $\cdot$ N. Wright (UCLA, USA) $\cdot$ R. Wyse (Johns Hopkins University, USA) $\cdot$ G. Zamorani (INAF OABO, Italy) $\cdot$ A. Zacchei (INAF OATS, Italy) $\cdot$ W. Zeilinger (U.Wien, Austria) $\cdot$ F. Zerbi (INAF Brera, Italy)

gravitational instability driven by dark matter. The standard cosmology also makes testable predictions about how the dark components affect the rate of expansion of the Universe and the development of its visible structures which can be discriminated with high precision only using newly developed technology on spacecraft. In this framework, we designed a new space mission aimed at addressing the key questions of modern cosmology. This study led to a proposal that was submitted to ESA in response to the call Cosmic Vision 2015-2025. The proposed mission was named *SPACE* : the *SPectroscopic Allsky Cosmic Explorer*. *SPACE* aims at producing the largest three-dimensional evolutionary map of the Universe over the past 10 billion years by taking near-IR spectra and measuring redshifts of $> 0.5 \times 10^9$ galaxies at $0 < z < 2$ down to $AB \sim 23$ over 3π sr of the sky. In addition, *SPACE* will also target a smaller sky field, performing a deep spectroscopic survey of millions of galaxies to $AB \sim 26$ and at $2 < z < 10+$. More information about *SPACE* can be found at http://urania.bo.astro.it/cimatti/space.

2 The *SPACE* key science case : Dark Energy and Cosmology

The acceleration of the Universe expansion is one of the most important discoveries of cosmology ([37], [35]). Both of the extant explanations for accelerating space-time require new physics: a negative pressure component dubbed dark energy, or a modification of the law of gravity and, therefore, the standard framework underpinning cosmology. The first possibility, dark energy, is currently favoured but, nevertheless, provides little help because we have no plausible candidates from elementary particle theories ([32]). The simplest expression of negative pressure is the cosmological constant, Λ. Unfortunately, there is no theoretical justification for the size of the cosmological constant as inferred from the rate of universal acceleration. The standard model of particle physics yields values between 10^{50} and 10^{123} times larger than the observed value. The cosmological constant is only one of several candidates to explain the acceleration of the universe. Most possibilities can be parameterized by their equation of state, the ratio of the pressure exerted by the dark energy to the energy density of the field: $w = P/\rho c^2$. A cosmological constant necessarily implies $w = -1$. The simplest alternative quantum-field explanations allow w to differ from -1 and to vary with time. Translating from linear time to observable redshift, z, we can parameterize $w(z) = w_0 + w_a(1-a)$, $a = 1/(1+z)$. The magnitude of w determines the rate of acceleration (through the associated pressure), so it can be characterized by measuring the rate of acceleration as a function of time for the history of the Universe, or equivalently, the Hubble parameter as a function of redshift, $H(z)$. Alternatively, the acceleration could be the result of a modified form of gravity, such as gravity that is a function of scale (e.g. [9]), or a modification of the standard model through string or brane theories (e.g. [33]). Distinguishing between dark energy, modified gravity and different variants necessarily requires high-precision measurements of the cosmic expansion rate history $H(z)$, but the remaining differences among

theories mean that even a very accurate $H(z)$ is inadequate to uniquely isolate one theory (e.g. [51]; [53]; [23]). The degeneracy occurs because a dark energy model and a modified gravity theory can give identical cosmic expansion histories $H(z)$, but would give very different growth histories of cosmic large scale structure ([25]). However, the predicted growth rate of large-scale structures varies among theories, and a measurement of structure evolution can isolate the correct one. The best current constraints on w from observations of distant supernovae are consistent with a cosmological constant: $-1 < w < -0.85$ with $10\% - 20\%$ uncertainties assuming a flat Universe ([62]; [38]; [41]). *SPACE* will determine $H(z)$ and constrain w_0 and w_a by combining the observations of the Baryonic Acoustic Oscillations (BAO), the growth rate of structures, distant Type Ia Supernovae and high redshift galaxies clusters.

### 2.1 *SPACE* and Baryonic Acoustic Oscillations

Baryonic acoustic oscillations (BAO) are small amplitude (5-10%) modulations in the distribution of matter imprinted at the epoch when matter and radiation decoupled ($z \sim 1000$). These ripples correspond to sound waves in the primordial photon-baryon fluid. The length scale of the oscillations is closely related to the sound horizon at decoupling, a scale (~ 150 Mpc) which is accurately known from measurements of CMB temperature fluctuations ([49]). This physical scale will have different apparent sizes on the sky at different redshifts and in different cosmologies. Assuming that distribution of galaxies reflects the distribution of all matter, this physical scale is measured from the spatial correlation (i.e. the power spectrum) of galaxies. The BAO technique derives its power from the patterns of high density that are frozen into the distribution of matter when it decouples from the photon background around the time of recombination. Acoustic patterns imprinted on the cosmic microwave background have provided the most precise measurements of cosmological parameters by the WMAP explorer and form the basis for even more precise measurements anticipated for the Planck telescope. It is precisely these kinds of patterns that are imprinted upon the distribution of matter, seen through the distribution of galaxies, that allow us to use them as standard rulers to measure $H(z)$. The acoustic oscillation length is effectively a standard ruler whose apparent size can be measured in the transverse and the radial directions (3D) from the distribution of galaxies. Combining the apparent size with the known physical size gives the distance at the redshift of observation and makes it possible to determine the expansion rate as a function of redshift, $H(z)$ ([5]; [17]; [45]; [58]). This technique is the most promising of the new methods proposed to measure the evolution of the expansion rate and therefore the relative effects of dark energy and dark matter. The astrophysical effects which may cause deviations of the ideal BAO signature, for example nonlinear evolution of the density field, dynamical redshift-space distortions, galaxy biasing are now well understood from numerical calculations ([45], [46]; [3], [4]; [12]; [18]). Angulo and collaborators ([4]) demonstrated that the pri-

BAO performance for constant w
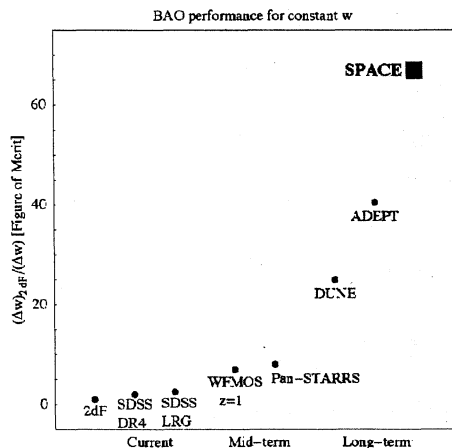
Fig. 1 The BAO performance of several surveys normalized to the 2dF in the case of a constant w (i.e. $\Delta w = \Delta w_0$ and w_a=0). The figure of merit is as defined by the Dark Energy Task Force. SPACE outperforms every other project for BAOs and also provides a rich dataset useful for complementary studies.

mary limitation on the accuracy of the BAO method is sample variance. Thus, to minimize the uncertainty in w, the observations need simply to maximize the survey volume. The application of BAO to extant galaxy surveys has already yielded constraints on w with uncertainties of only 10% (e.g. [11]; [19], [20]; [52]; [34]) even though this technique is only a few years old. To maximize the sample volume, *SPACE* will perform a spectroscopic All-Sky Survey to measure galaxies over 3/4 of the entire sky and over the redshift interval $0 < z < 2$, centered on the redshift $z \sim 1$ at which the dark energy first starts to dominate the expansion of the Universe. The sensitivity requirement is $SNR \sim 3$ per resolution element at $H_{AB} \sim 23$. Taking spectra at near infrared wavelengths ensures that *SPACE* covers the entire redshift range efficiently. The use of a space-based multi-object spectrometer makes it possible to get accurate redshift of millions of galaxies over the whole sky in a short time. The evolution of the dark energy will be measured by dividing the sample into redshift slices of width $\Delta z \sim 0.5$ each and measuring the BAO signature in each slice (Figure 1). Recent works emphasized the need to trace $w(z)$ with high accuracy in order to derive the most stringent constraints on the Dark Energy (see [23]). *SPACE* should achieve 0.5% accuracy in the BAO scale measurement from these redshift slices. The best constraints on dark energy will result from a combination of complementary datasets (Figure ??. But also in the case of *SPACE*"alone", the cases of (*Planck*+ *SPACE*BAOs), (*Planck*+ *SPACE*BAOs + current SNe) and (*Planck*+ *SPACE*BAOs + *SPACE*SNe) will provide constraints on $w \approx 5$, ≈ 10, and ≥ 20 times more accurate than the current accuracy. This also highlights the "self-sufficiency" of *SPACE*.

SPACE fully meets the requirements of the Dark Energy Task Force (DETF) (http://home.fnal.gov/ rocky/DETF/) which recommended that the goal for new survey designs should be that their "Figure of Merit improves by a factor of three between different Stages of dark energy missions" ([1]). Com-
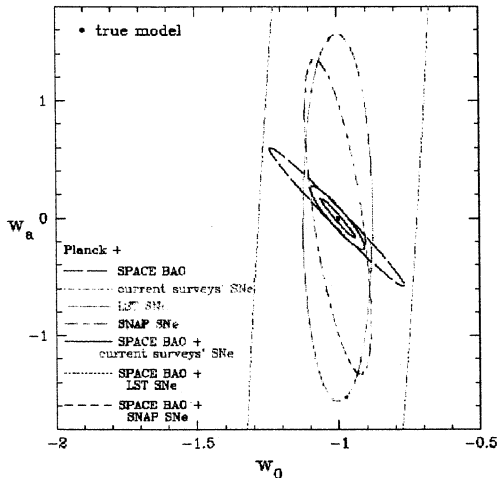
Fig. 2 The joint 68% confidence interval constraints on the dark energy equation of state parameter (w_0) and its evolution with redshift (w_a). Several datasets can be combined to improve the constraints. SPACE will dramatically improve our knowledge of w_0 and w_a.

bining the *SPACE* BAO measurement with a "long-term Stage IV experiment (LST, JDEM, SKA) produces a further factor of three gain in the constraints on dark energy. Thus, *SPACE* falls in the next category of so called Stage V experiments.

2.2 *SPACE* and the Growth Rate of Cosmic Structures

The growth rate of cosmic structures due to gravitational instability offers the capability to distinguish between different theories that produce the same $H(z)$ and provides an independent and novel probe of the nature of dark energy or possible modifications to gravity. The growth rate $f_g(z)$ can be measured from the impact of gravitationally induced peculiar motions (i.e. motions of galaxies in their local rest frame relative to the systemic flow due to the Hubble expansion) on the pattern of galaxy clustering. These motions produce an anisotropy in the galaxy redshift-space correlation function, $\xi(r_p, \pi)$, in directions parallel and perpendicular to the line of sight. The coherent bulk flows towards overdensities lead to an enhancement of the clustering signal on large scales, quantified as a compression in the iso-correlation levels of $\xi(r_p, \pi)$. The compression is directly proportional to the value of $f_g(z)$, modulo the *bias factor* of the objects used to trace the matter distribution, b, measured by the parameter $\beta = f_g(z)/b$ (e.g. [16]). The feasibility of this technique at intermediate redshifts has just been demonstrated in an important breakthrough using the VVDS redshift survey and by measuring β with 40% uncertainty from an area of 4 deg^2 using 6000 galaxy redshifts over a wide redshift range ([15]; [36]). Other recent studies emphasized the power of this approach for differentiating between dark energy and modified gravity ([24], [59]).
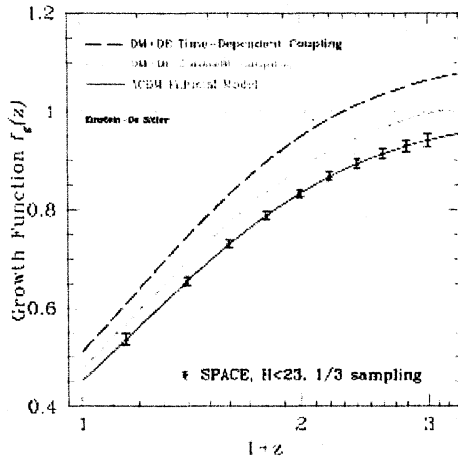
Fig. 3 The predicted performance of SPACE in measuring the growth rate of density fluctuations as a function of redshift, $f_g(z)$ using the anisotropy of galaxy correlations, assuming a ΛCDM fiducial model. SPACE will disentangle to high accuracy the cosmological constant theory from variants of dark energy (here two possible cases are shown - [2]). The combination of the fully independent measurements of $H(z)$ from BAOs and $f_g(z)$ from redshift distortions will provide a direct test of whether cosmic acceleration is due to a modification of Einsteins theory of gravitation or to new physics beyond the standard model.

SPACE will make a dramatic improvement, thanks to enormous volume sampled, even in slices of $\Delta z = 0.2$, and to the deep infrared selection ($H < 23$), that allows the $N(z)$ to extend significantly above $z = 1.5$, with a mean density always larger than ~ 0.02 gal h^3Mpc^{-3} to $z \sim 2$ even with a sampling of 1/3 galaxies. Our simulations clearly show that *SPACE* will be unique in providing a precision measurement of the growth history of cosmic structures, reaching 0.5% accuracy in β in redshift slices of $\Delta z = 0.2$, and measuring directly the growth function $f_g(z)$ to 1% accuracy (Figure 3). The bias factor (b) will be extracted in each redshift slice using higher-order galaxy clustering ([56]) or via self-consistent density-reconstruction methods (e.g. [47]).

2.3 *SPACE* and distant Type Ia Supernovae

Using Type Ia Supernovae (SNe Ia) as standard candles to measure H(z) is the method by which the existence of dark energy was first discovered ([37]; [35]). *SPACE* observational strategy can be designed to allow the discovery of SNe Ia and to obtain their spectroscopic redshifts out to $z \sim 2$ very efficiently thanks to the simultaneous multi-object spectroscopy over a wide field. For instance, the observation of a 4 deg^2 Deep Field ($H < 26$) would allow the identification of ~ 2300 SNe to $z \sim 2$ in about 4.8–6.5 months spread over 1 year, where 1 visit would take 4 days to cover 4 deg^2 to $H \sim 26$, and each visit would be repeated every 7–10 days. With such a strategy, *SPACE* would obtain roughly the same number of SNe expected for SNAP to $z = 2$ in 1/5 of time. We also note that near-IR spectroscopy is advantageous because less affected by dust extinction, and hence very useful for high-z SNe. One could imagine an ideal scenario where SNAP and *SPACE* are operational in the same time frame in order to provide the strong synergy with SNAP discovering SNe

through imaging and *SPACE* identify them with spectroscopy. The details of the *SPACE* -SNe program will depend on the developments of other future projects in space and on the ground (e.g. SNAP, Pan-STARRS, LSST, ...)

2.4 *SPACE* and high-redshift galaxy clusters

Galaxy clusters are the end products of the hierarchical build-up of small systems into increasingly larger structures up to 10^{15} $M_\odot$. Since clusters arise from rare high peaks of primordial density perturbations, their number densities and mass distribution, i.e. their mass function $n(M, z)$, is highly sensitive to the matter density parameter Ω_m, and dark energy parameters (Λ, w) which control the rate at which structure grows, as well as to the normalization of the matter power spectrum, σ_8. At $z > 1$, the existing surveys do not yet place strong constraints on dark energy due to the small volumes probed and because only a handful of systems have been identified to date (e.g. [39], [31], [50]). *SPACE*, with its unmatched spectroscopic speed in near-IR, will provide spectroscopic confirmation of all the thousands of clusters at $z > 1$ detected in the next generation near-IR, Sunyaev-Zeldovich (SZ) and X-ray large area surveys (e.g. SPT in 2007+, Planck in 2008+, eROSITA in 2012+). *SPACE* will identify bona-fide virialized structures, the ones to be compared to the theoretical cluster mass function, and it will resolve the cases of contamination from point-like radio sources and AGN that are expected to plague future SZ and X-ray searches for distant clusters. Thus, *SPACE* will unleash the full potential of the next generation cluster surveys by allowing the best possible knowledge of systematic errors, with small statistical uncertainties limited only by the volume of the observable Universe. We recall that constraints from cluster surveys generally exhibit parameter degeneracies different from those of other techniques, such as CMB, Type-Ia SNe and BAO described above. The pursuit of these complementary means, based on different physical properties of the Universe, is the most powerful way to unveil the nature of the dark energy and dark matter. In addition, *SPACE* itself will locate for the first time several tens of thousands of clusters directly in three dimensions out to $z \sim 2.5$ and over a large mass range.

3 From Dark Matter to Baryons: the Formation and Evolution of Galaxies

In the standard model of galaxy formation, galaxies coalesce from gas that cools inside dark matter halos ([60]). Determining the physical processes that regulate the growth of galaxies and their link with massive black holes is one of the outstanding problems of modern astrophysics. By observing galaxies down to faint magnitudes and sampling one of every three of these faint galaxies, *SPACE* will measure the characteristics of more than half a billion galaxies as a function of their environment at sensitivities impossible to obtain from ground-based telescopes. We take this opportunity to underline why *SPACE* must

observe in the near-infrared. The strong optical-ultraviolet spectral features of galaxies well below L_* that are primary redshifts and diagnostic tracers fall, in the redshift range $z \sim 0.5 - 3$, in the near-IR. Their list includes: Balmer and D4000 continuum breaks, strong H Balmer lines, CaII H&K lines, as well as the well-studied diagnostic emission lines such as [O II]λ3727, Balmer lines, [O III]$\lambda\lambda$4959,5007, and several high ionization lines useful for identifying the presence of an active galactic nucleus. At higher redshifts, *SPACE* will obtain redshifts and diagnostics of the young stellar populations and the interstellar medium using rest-frame ultraviolet lines.

The reason why it must be done from space is also clear: 30% of the wavelength range between 1 and 2 μm is invisible from the ground, and for the remaining fraction the bright and variable night sky lines dominate (at the $\sim 95\%$ level!) the background. At low spectral resolution ($R \sim 500$), their filling factor is virtually 100%. Even at $R \sim 2000$, less than half the near infrared spectral range is free from night sky line emission ([?]). These emission lines, variable in intensity on time scales of minutes, add background noise, subtraction residuals and scattering that make cosmic line and redshift determination of faint sources from the ground nearly impossible, no matter how long one integrates. *SPACE* combination of wavelength coverage, resolution and sensitivity will remove the degeneracy limiting the photometric SED fitting (reddening vs. red stars). A list of what *SPACE* will be able to accomplish includes: (1) to provide a complete census of galaxies independent of their type and measure the evolution of the distribution functions with the highest accuracy possible and limited only by cosmic variance (e.g. luminosity, stellar mass) significantly below the characteristic mass, M_* (for example, *SPACE* will observe passive galaxies from $z = 1.5$ to their formation epoch), (2) to investigate how the properties of galaxies depend on the density of their surroundings, (3) to determine the merger rate as a function of redshift, (4) to determine black hole masses from line widths and compare them to the stellar content, mass, and age of the host galaxy, to directly probe feedback processes in the largest high-z sample of AGN ever, (5) to determine the causes of downsizing, whereby star-formation histories correlate with stellar mass, and the active sites of star-formation move to increasingly higher mass galaxies with redshift, (6) to provide a unique resource for measuring all aspects of the spatial distribution of galaxies and clusters on smaller scales, including the higher order correlation functions (i.e. the amplitudes of the N-point correlation functions) which are sensitive to the growth of structure through gravitational instability and offer a direct route to measuring galaxy bias (see section 2.2). Moreover, *SPACE* will enable new facilities such as LOFAR, eROSITA, WISE, SKA to reach their full capability by removing the significant bottle neck in obtaining the redshifts for the large survey samples.

4 Galaxies and QSOs in the early Universe

In the area of galaxy and AGN co-evolution, *SPACE* will provide a unique contributions through a spectroscopic Deep Survey, targeting galaxies at redshifts as high as 10, when the Universe was a few hundred million years old. The *SPACE* Deep Survey will be designed to study large samples at high redshifts following a strategy of this type: (1) Z-, J- and H-band imaging of a 10 deg^2 area to $H = 26^m$, $J \sim 28^m$, $Z \sim 28^m$, (2) narrow-band imaging of the same area, (3) spectroscopy to $H = 25^m$ over the same area and with a sampling rate of 90% (mostly at $2 < z < 7$), (4) the candidates at $z > 7$ will be pre-selected from broad-band colors ([8], [7]) using the *SPACE* imaging data themselves and will be repeatedly observed for secure spectroscopic identification. Based on the observed galaxy luminosity function at $z = 6$ ([7]), extrapolated at higher redshift under the assumption of simple luminosity evolution, in an area of 10 deg^2, there will be ~ 800 galaxies at $z > 7$ with $H < 26^m$, ~ 500 at $7 < z < 8$, ~ 200 at $8 < z < 9$, and a few tens above $z = 9$. As the most massive objects at these redshifts are extremely rare, the large FOV of *SPACE* compared to JWST gives it an enormous advantage: only ~ 0.3 massive galaxies should be present in the JWST field of view of ~ 10 arcmin^2. *SPACE* is the natural complement to JWST for the study of high redshift galaxies. With narrow-band filters, it will be possible to search for Ly-α emitters too faint to be detected in the broad-band *SPACE* images by selecting objects showing an excess of flux in narrow-band filters with respect to the broad-band one. For instance, filters centered at ~ 1.03 and ~ 1.34 μm, allowing an extensive Ly-α emitter search at $z \sim 7.7$ and $z \sim 10$. At $AB = 26$, *SPACE* should find ~ 1200 (~ 30) emitters at $z \sim 7.7$ ($z \sim 10$) objects with Ly-α fluxes as low as $\sim 4 \times 10^{-18}$ erg s^{-1}cm^{-2} with $S/N \sim 10$. A fraction (up to 10%) of these sources is expected to be powered by very massive, metal-free stars, the so called Population III stars ([42]). These objects can be selected from *SPACE* data owing to their very large Ly-α equivalent width and He II $\lambda 1640$ emission ([43]). Finally, *SPACE* will also obtain the definitive measurement and spectrum of the so far elusive cosmic Near Infrared Background (NIRB) (e.g. [21] and references therein). Sources at $z > 5$ contributing to the reionization of the Universe are expected to produce a strong feature in the NIRB, with a well defined maximum at $\sim 1\mu$m with $\nu I_\nu \sim 1$ nW m^{2}sr^{-1} and a strong break below 1 μm due to the strong absorption by the intergalactic medium (IGM) below rest-frame 912 Å([40]; [10]).

The enormous sky coverage of the *SPACE* survey will also reveal several hundred QSOs at $z > 6$ (including a few tens of objects at $z > 9$) and shed light on the evolution of supermassive black holes. For instance, if we adopt the currently known luminosity function (LF) at $z = 6$ ([13], [61]) and the target sampling rate of 1/3 of the *SPACE* all-sky survey, we find that $120, 90, < 1$ ($40, 20, < 1$) QSOs are expected at $z > 7$ ($z > 9$) in case of no evolution of the LF, linear evolution with SMBH masses decreasing linearly (from $z = 6$) with look-back time, and Eddington evolution with SMBH masses decreasing exponentially with an e-folding time $\tau = 45$ Myr. The *SPACE* spectral reso-

lution is good enough to study the absorption of photons from Lyα and Lyβ transitions through the IGM as a function of redshift. The masses of QSOs can be measured from the *SPACE* spectra using the C IV λ1549 Å line ([?]). Currently, it takes about 8 hours with Keck 10m telescope to obtain a suitable near-infrared spectrum of a QSO at $z \sim 6$ (e.g. [48]), whereas in 15 minutes *SPACE* would go 3 magnitudes fainter. Before 2017, programs on ground-based telescopes will search for high-redshift QSOs by imaging in several optical and near-infrared bands, and using drop-out techniques. Such techniques are limited by (a) the near-infrared imaging depth achievable from the ground for a large sky area, (b) the limited redshift ranges available to the drop-out technique, (c) the large fraction ($> 95\%$) of drop out candidates that are cool stars, and (d) the OH sky lines covering $> 40\%$ of the near-infrared spectrum. Ground-based surveys are expected to find only a relatively small number of high-redshift QSOs (for a recent example of the process, see [55]). For a significant increase in the number of objects, and to really open up the unexplored redshift range ($z > 7$), we need to search for high-redshift QSOs over the entire available all sky with spectra that cover a large wavelength range free from by atmospheric emission lines.

5 The Near-Infrared view of our Milky Way Galaxy

At low galactic latitudes source crowding represents a problem for multi-slit spectroscopic surveys. However, the extreme versatility of the instrument we have envisioned allows us to perform integral field spectroscopy using coded masks (Hadamard transforms). A *SPACE* Galactic-plane survey will be feasible with a relatively modest investment of time by covering in integral field mode the strip within $\pm 0.5°$ centered on the Galactic Equator between $\pm 60°$ of galactic longitude to magnitude $AB \sim 20$. Other examples of key contributions of *SPACE* in Galactic studies will be the census of ultracool dwarfs in the vicinity of the Sun and the estimate of the lower mass function in star-forming regions.

6 Simulations

In order to assess the mission feasibility and efficiency, and to define the most suitable characteristics of the instrumentation, the performances of *SPACE* were extensively simulated in details both for imaging and spectroscopy.

6.1 Spectroscopy

In the case of spectroscopy, we explored different instrument configurations using the VVDS slit positioning software ([6]) and using both real and artificial (from the Millennium Simulations) galaxy catalogs with magnitudes matched
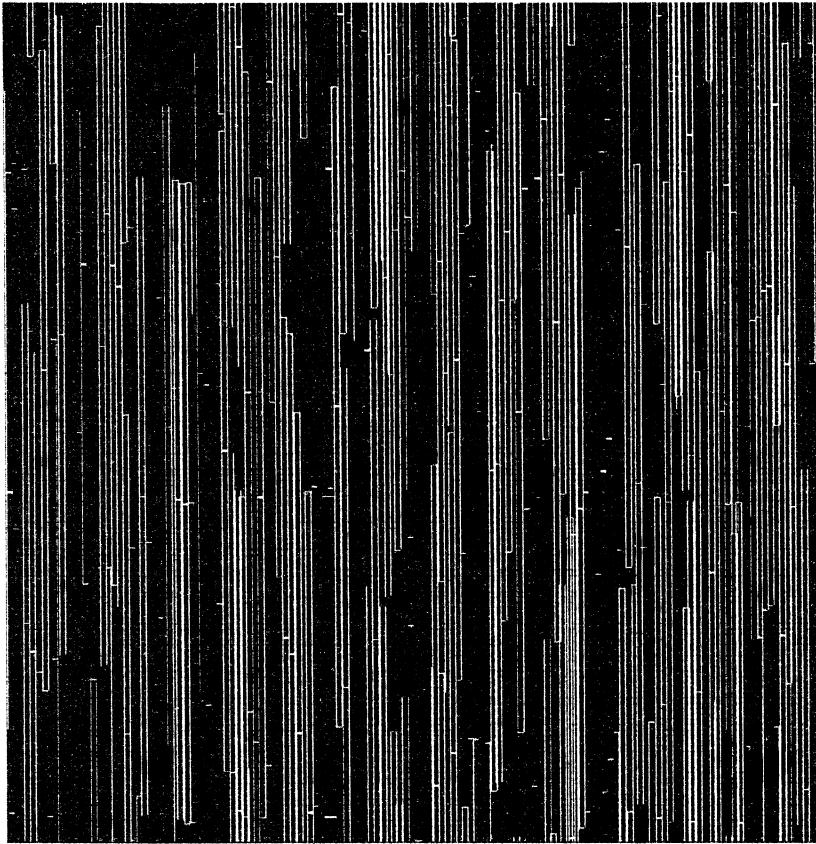
Fig. 4 A simulated 5 × 7 field showing the location of the spectra of the selected targets.

to the sensitivity limits of the All-Sky and Deep Survey. The software does not allow the overlap of spectra both in the spatial and in the wavelength directions. The mission efficiency was evaluated as a function of instrumental parameters and galaxy properties, conservatively allowing 2 empty pixels between spectra to accommodate spectral distortions. The best results are obtained with: 4k×4k detector, pixel size 0.375″, 15 Å/pix dispersion, 2 pixels per DMD along dispersion, spectrum length of 670 pixel, spectral resolution of 400. This combination allows a sampling of 1 of every 3 galaxies to $H = 23^m$(AB), giving a 31% efficiency.

With the above parameters, we simulated spectra including background and detector noise. Template spectra ([22], [28], [44]) of a variety of galaxy types (early-type, star-forming, starbursts, AGN, Lyman-break, etc.) provided the input to the simulations as a function of the magnitude and redshift for a total of about 180,000 spectra at $0.2 < z < 2.4$ for the all-sky survey ($H < 23$)
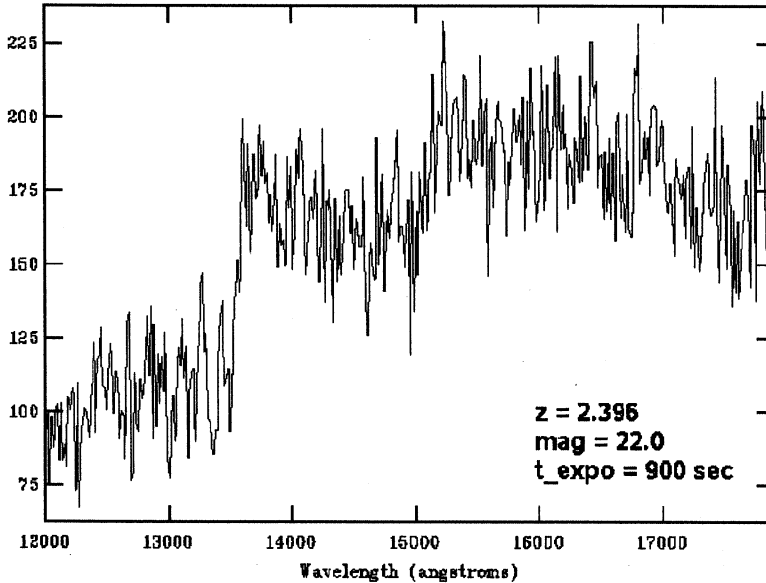
Fig. 5 Simulated spectrum of an early-type passive galaxy at $z > 2$. The D4000 break and the main absorption lines (CaII H&K) are clearly detected. It is impossible to obtain such a spectrum with ground-based near-IR spectroscopy due to the sky background, OH line contamination and telluric absorptions.

and about 1,000 at $2.4 < z < 10$ for the Deep Survey ($H < 25 - 26$). The results show that the dispersion and the resolution of *SPACE* are adequate to reliably identify the main emission and absorption features of all galaxy types (Figure 5). Redshifts have been automatically measured with EZ (the software tool used in VVDS and zCosmos projects) and other tools specifically developed for the simulations. The low background, wide wavelength coverage, and moderate spectral resolution produce a success rate of spectroscopic redshift measurements between 80%–99% for the planned integration times of 900 sec (All-Sky Survey) and 7 hours (Deep Survey) for all galaxy types and redshifts. The typical accuracy on individual redshifts $\sigma_z = 0.001$. In comparison, with the same integration time of 900 sec, slitless spectroscopy would provide a S/N ratio about 10 times lower.

6.2 Imaging

We verified that the photometric catalogues derived from *SPACE* imaging will provide high quality target lists for the spectroscopic observations. We used the NICMOS H-band observations of the Hubble Ultra Deep Fields (HUDF) with PSF $FWHM \sim 0.15''$ to match closely the PSF delivered by the 1.5m

SPACE mirror and resampled the data at the *SPACE* scale of $0.375''$/pixel. The vast majority of sources detected in this image, reaching well beyond $H = 27^m$, are still easily seen in the resampled image without blending or confusion. We measured blending and confusion as a function of magnitude using source detection software for the original and resampled HUDF images. The results are: (1) at the $H < 23^m$ (all sky survey), 97% of the sources are still individually detected in the resampled image, (2) at $H = 26^m$, only $\sim 15\%$ of the sources appear blended with neighbouring sources, (3) source counts from the original and resampled image are consistent up to well beyond $H = 26$.

7 The *SPACE* science programmes

The main objective of *SPACE* will be to execute a Core Science Program in about 3.5 years. However, given the power and flexibility of *SPACE* in many fields of astrophysics, it will allow also for Guest Observer Science Programs. The Core Program will be composed by:

– The *SPACE* all-sky survey; it will observe the entire sky at galactic latitudes $> \pm 18°$ ($\sim 70\%$ of the total). This corresponds approximately to 28,500 square degrees and 71,000 satellite pointing (1 pointing = $0.4 \deg^2$). Assuming 20 minutes per pointing and an observing efficiency of 75%, this will require 2.7 years. The expected number of galaxy spectra with a 1/3 target random sampling is $(50,000/3) \times 71,000 \times 0.4 \sim 0.5 \times 10^9$. The selection of the spectroscopic targets will be done taking an acquisition image in the H-band at $AB \sim 23.5$ immediately before the spectroscopic observation. Targets will be selected using onboard software, following the approach currently adopted in ground-based spectroscopic surveys (e.g. VVDS, zCOSMOS). As a byproduct, the acquisition images will produce the deepest all-sky imaging survey at $|b| > \pm 18°$.

– The *SPACE* Deep Survey; it will target a 10 $\deg^2$ field (25 *SPACE* pointings) down to $H(AB) = 25^m$, with a target sampling rate of 90%, and without any color pre-selection. About 200,000 objects (stars+galaxies) are expected in 1 $\deg^2$ at $H < 25$. With a multiplex of ~ 6000 objects and an integration time of about 7 hours per observation to reach a sufficient S/N, we need $\sim [(200,000 \times 0.4 \times 0.90)/6000] \times 25$ pointings $\times 7h \approx 5$ months. We recall that the $z > 7$ galaxy candidates will be pre-selected using the *SPACE* imaging in z,J,H bands and will be compulsory targets repeated in each of the 12 spectroscopic observations done for each of the 25 pointings so that they will accumulate a total integration time of (7 h$\times$12) = 84 hours (per pointing) needed to reach a sufficient S/N for J, H = 26. The time needed for the broad-band z-, J- , H-band and narrow-band imaging will be negligible with respect to the time dedicated to spectroscopy. With an appropriate strategy of repeated visits, the Deep Survey could be used also for detecting high-z SNe.

- The *SPACE* Galactic-plane survey; it will cover in Integral field mode the strip within ±0.5° centered on the Galactic Equator between ±60° of galactic longitude. We will allocate 4 hr per pointing, i.e. 10 hours per square degree and 50 days total for the entire survey.

Allocating a fraction of the time to a Guest Observer Program will add value to the mission. We will split the Core Science program in a four phases lasting approximately 9 months each, allowing the GO observing time to be ramped up over time in a manner similar to the phasing in past missions such as ISO and Spitzer. This will allow the core science program to be completed in a timely manner while providing the community with early instrument performance information and science results to use in the planning of observations for other studies.

8 *SPACE* Mission concept

8.1 Driving requirement

The science requirements identified in the previous sections place firm constraints on the mission concept and the design of the instrument.

The first need is to access to the whole celestial sphere for about 3 years. The core observing program requires $0.1''$ pointing stability for at least 30 min of typical integration time, high temperature stability and good access to the ground station for data downlink and telemetry. All these requirements are ideally met by a large-amplitude halo orbit around the second Earth-sun Lagrange point (L2). A halo orbit at L2 maximizes the availability of the sky for observation with respect to the visual and thermal disturbance from the Sun, Earth and Moon. The thermal environment is very stable and, with the exception of solar storms, the radiation environment is low. On a halo orbit of sufficient amplitude eclipses can be avoided altogether, while the constant satellite-sun-Earth geometry eases the thermal control and the communications. L2 is considered the ideal vantage point for an IR observatory and several mission (e.g. Herschel, Planck, GAIA, JWST) will be operated at L2.

In order to measure a large number of sources, one needs multi-object spectroscopic capability over an area of the order of 1 square degree. In order to observe faint sources, one needs to operate in slit mode, exploiting the celestial background from space ~ 500 times lower than from the ground. The sensitivity requirement also drives the telescope diameter, whereas the large field of view drive the effective focal length of the optical system. The broad wavelength range and resolution of the spectrograph drives the choice of materials (mirrors vs. lenses), the detector technology, the instrument temperature, and ultimately the multiplexing capability of the instrument. In particular, the need for extensive multi-object capability suggests considering Micro-Electro-Mechanical-Systems (MEMS), following the approach pioneered for NIRSPEC on JWST ([30], [26]).

Having set through performance simulations the basic requirements on the instrument parameters (see Sect. 8), we have evaluated several possible solutions and converged finally on an elegant design that satisfies all requirements. To keep complexity and cost to a minimum we aimed for a single-mode instrument rather an all-purpose machine with a variety of arms and configurations. Nevertheless, we came out with a solution which inherently provides an extraordinary degree of versatility without adding complexity, weight or cost to the basic hardware needed for our main survey program. Using MEMS for target selection we have several millions of randomly addressable optical switches. Depending on the MEMS configuration, and on the selection of a filter or a prism in a filter wheel (the only moving part) *SPACE* can perform imaging, slitless and slit spectroscopy (our main observing mode), and even wide-field integral field spectroscopy using Hadamard transforms.

8.2 Payload description

The *SPACE* payload is a compact and modular instrument, fitting below the primary mirror structure within a cylindrical envelope of 1.5 m diameter (the size of the primary) by 60 cm height. To accommodate for our large field of view, the beam is split into 4 identical channels, each one taking a 90° sector of the cylinder. Each channel is a relatively conventional spectrograph with a MEMS device located at the intermediate focal plane. For the MEMS device we have opted for a Texas Instrument DMD of 2048×1080 micro-mirrors, whereas for the detector we use a $4k \times 4k$ infrared Focal Plan Assembly similar to the one developed for JWST. Each micro-mirror images a square $0.75'' \times 0.75''$ field onto 2×2 detector pixels. Hereafter we will examine the main component of a spectrograph more in detail

1. The telescope is a Ritchey-Chrétien F/5.83, with a 1.5m F/2.7 primary. A Ritchey-Chrétien telescope, in which both mirrors are hyperbolic, is free from coma and allows for easy optical testing.
2. The telescope focal plane falls on a 4-face pyramid mirror providing a total coverage of $51' \times 27'$ (~ 0.4 square degrees). The layout sketched in Figure 7 preserves the symmetry around the optical axis allowing the four channels to be identical with substantial cost saving in the design, fabrication and testing. It still allows to tile the sky with multiple contiguous observation to map large fields without significant losses in coverage.
3. Each subfields of the pyramid mirror is reflected toward a fore-optics system, made of 4 mirrors (Figure 8) contained in a layer ~ 400 mm deep under the primary support structure. The fore-optics system projects on the DMD an undistorted image of the focal plane with a scale of $0.75''$/DMD facet and excellent optical quality.
4. The DMD micro-mirrors are 13.6 μm on a side and tilt along their diagonal by $\pm 12°$. When the DMD facets are tilted to their ON position, the beam is reflected in a direction approximately normal to the DMD plane, while
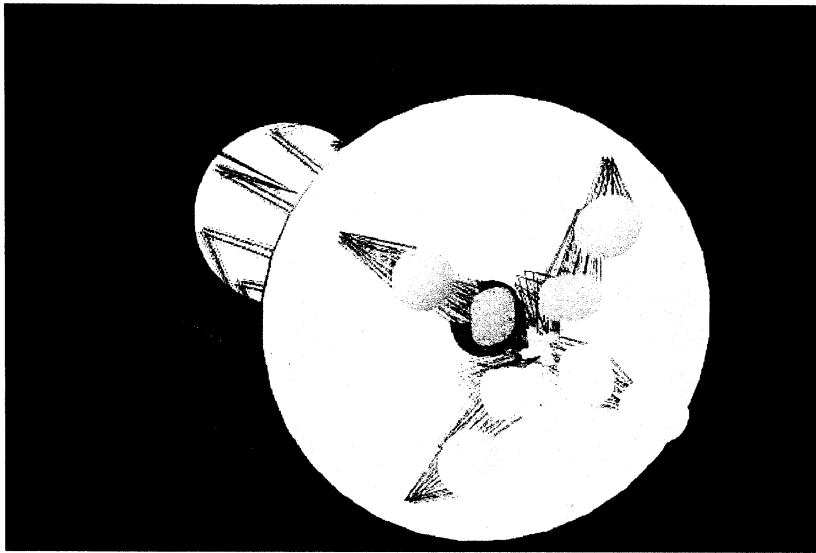
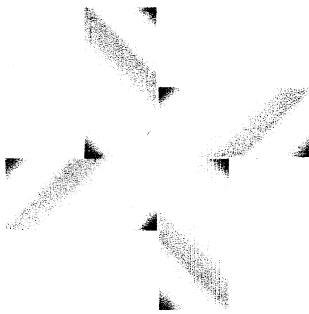**Fig. 6** Optical Telescope Assembly and fore-optics system (four channels).

Fig. 7 Four-fold symmetric cross for the SPACE pyramid mirror allowing for 4 identical optical channels.
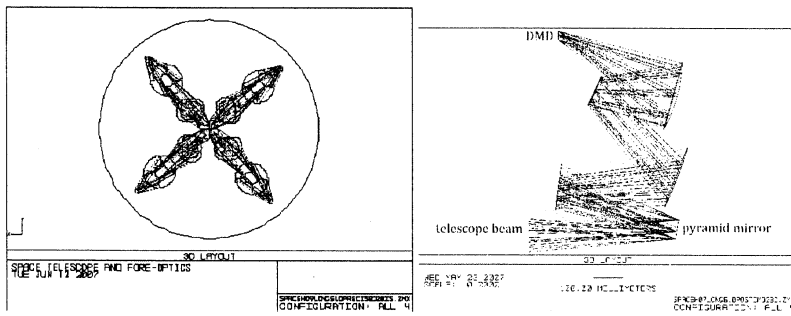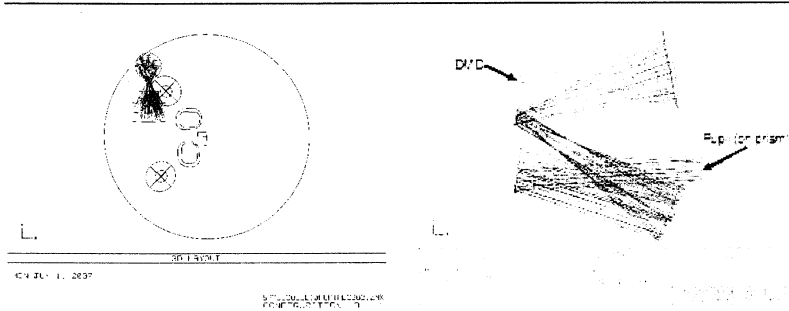

**Fig. 8** Fore-optics system. Left: top view (all channels); Right: side view (one channel).

Fig. 9 Left: top view layout of the collimator (one channel). The location of the fore-optics mirrors of two channels (Figure 8) is also shown to illustrate the different orientation of the collimator (along a cord) with respect to the the fore-optics (along a radius) after reflection on the DMD. Right: side view layout of the collimator.

when they are turned OFF they reflect at an oblique angle towards a beam dump.

5. The collimator collects the beam reflected by the DMD relaying an image at infinity. Its design is similar to that of the fore-optics, with 4 mirrors located in the same 400mm thick layer (Figure 9). The collimator, however, develops inward along a cord rather than outward along a radius, therefore the incoming and outcoming beams do not cross. The collimator produces a 66 mm pupil located nearly on the same plane of the pyramid mirror.

6. The prism is located in the immediate vicinity of the pupil. Having set at $R \sim 400$ target, we have considered a number of solutions based on both grisms and prisms in different configurations and materials. Our final choice is for a single pass prism + folding mirror placed immediately after the pupil. For the imaging mode, the prism + folding mirror are substituted by a simple 45° folding mirror and broad-band filter. A single filter wheel per channel allows to insert the other required imaging filters (e.g. z, J, narrow band).

7. The camera reimages the DMD plane onto the detector plane with a 1:2 ratio, in pixel units. The camera has 4 lenses, including 2 aspheric surfaces, and is achromatic and diffraction limited between 0.6 and 1.8 μm. The length of a 0.8-1.8 μm $R \sim 400$ spectrum is ~ 670 pixels, slightly dependent on the field position. Thanks to a folding mirror, the detector can be located in the area below the pyramid mirror. Having all IR detectors located close to each other simplifies the cooling system.

8.3 Detectors

SPACE will utilize HgCdTe Focal Plane Arrays (FPAs). Teledyne devices, based on the Hawaii-2RG multiplexer, with long wavelength cut-off at $\sim$ 1.8 μm are ideally suited because of their modest sensitivity to the spacecraft
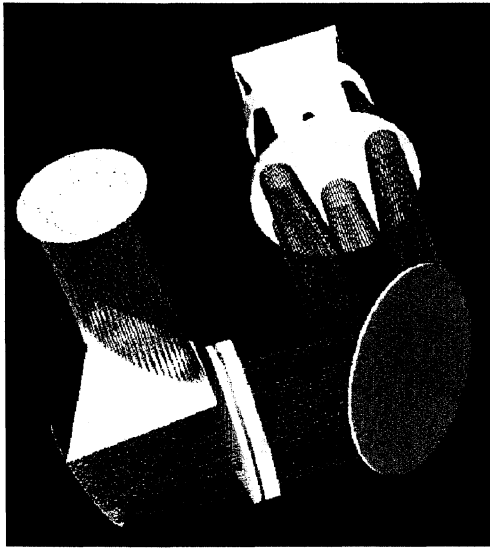
Fig. 10 Prism and camera 3-d layout. A 45° folding mirror can be inserted in the camera to relay the image in the most convenient position at center of the spacecraft.
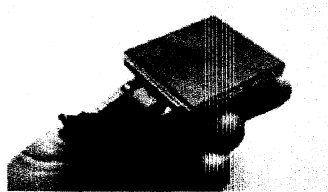
Fig. 11 A 2k×2k buttable Focal Plan Array developed for JWST.

thermal emission and to the low dark current levels exhibited at relatively high operating temperatures, $\sim 140 - 150$ K, but more conventional 2.5 μm devices can also be used, since the spacecraft will be passively cooled. This technology is mature. The IR channel of the HST/WFC3 camera is equipped with FPAs with 1.72 μm cutoff wavelength on a 1k×1k multiplexer. The most recent WFC3 parts attain $\sim 80\%$ QE nearly flat over a $1.0 - 1.70$ μm range, readout noise in double correlated sampling < 25 e/read and dark current ~ 0.01 e/s/pixel at 140 K. JWST devices for NIRCAM and NIRSPEC with 2.5 μm cutoff have also been produced in 2k×2k format, with excellent performance. Note that the substrate removal process, necessary to eliminate radiation induced glow, extends the spectral response down to 0.4 μm, allowing an extension of the wavelength range down to e.g. 0.60 μm that we are considering for *SPACE*.

These devices can be butted together in a $2 \times n$ configuration (Focal Plane Assembly, FPA). For *SPACE* we are considering 2×2 FPA similar to those developed for JWST, A 4k×4k assembly allows to easily accomodate for the extension of the spectra.
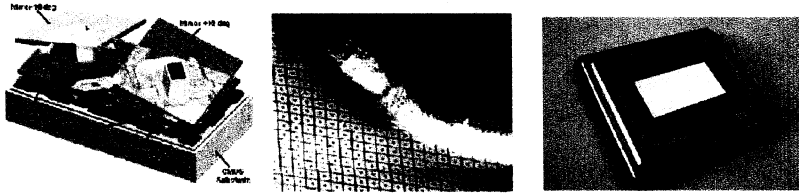
Fig. 12 Left: typical substructure of a TI DMD; center: DMD array with an ant leg for comparison; 3: packaged DMD CINEMA (2048×1080) device.

8.4 Digital Micromirror Devices (DMDs)

The innovative technical aspect of the *SPACE* mission is the use of DMDs. We have taken a fresh look at these devices, that were originally considered for NIRSPEC on JWST, and concluded that they represent the ideal choice for *SPACE*. Since their invention by L. Hornbeck at Texas Instruments (TI) in 1988, DMD have been serially produced with volumes exceeding 10 million units shipped by 2006. Today DMDs represent one of the leading technologies in digital imaging (e.g. DLP projectors). For this multi-billion dollar market huge investments have been made, reaching unique levels of quality and reliability. We intend to capitalize on these investments.

8.4.1 What are DMDs?

DMDs are a particular type of Micro-Electro-Mechanical Systems (MEMS). MEMS integrate microscopic mechanical elements, in our case moving mirrors, together with their control electronics on a common silicon substrate. Whereas the control electronics is fabricated using standard integrated circuit processes, the mechanical components are fabricated using "micromachining" processes that selectively etch away parts of the silicon wafer or add new structural layers. In the case of DMDs, the mechanical part is an array of up to 2.21 million aluminum micromirrors fabricated on top of a complementary metal oxide semiconductor (MOS) static random access memory (SRAM) array. Each micromirror, independently controlled, can switch along its diagonal thousands of times per second as a result of electrostatic attraction between the mirror structure and the underlying electrodes. The current generations of DMDs all exhibit a $+12°/-12°$ tilt angle, limited by a mechanical stop. Pixel pitch in currently available DMD is either 10.8 μm (0.6 μm gap width) or 13.68 μm (0.68 μm gap width) center-to-center. TI produces several types of DMDs in hermetic packages. Those with more than 2 million pixels are the 2048 × 1080 pixels CINEMA device (Figure 6.9.3) with 13.68μm pixel pitch, and the 1920 × 1080 1080p High Definition TV device with 10.6 μm pixel pitch. For our baseline design we have considered the former, but optical solutions can be found for smaller devices.

8.4.2 Why DMDs? (instead of micro-shutter arrays)

The main alternative to DMD is the Micro-shutter array (MSA), which has been developed and optimally matched to the IRMOS/JWST. MSAs represent an outstanding technological achievement and are especially unique in their capability of operating at low temperatures. However, they come in much smaller size (at the moment 171 × 365 pixels) and are still prone to cosmetic defects. Other figures of merit (e.g. filling factor, contrast, reliability) do not appear to be superior to those achieved by the current generation of commercial DMDs. DMDs are technologically mature, already in use in Astronomy ([27]) and meet all the optical and technical needs of the *SPACE* mission. The issues (optical quality, contrast, reliability, radiation environment, ...) related to the use of DMD in our mission are discussed in detail in the *SPACE* proposal.

## 9 Performance assessment with respect to science objectives

We have verified that with our proposed design *SPACE* reaches the sensitivity goals stated in the Sect. 6 and 7. Using the baseline optical design described in the previous section we have estimated the signal to noise ratio per resolution element in 900 s of integration (Fig. 6.6). A $SNR \sim 3$ at AB=23 is the sensitivity requirement derived in Section 3 for the All-sky survey. The sensitivity estimates for the Deep Survey are also compatible with the requirements.

10 Operating modes

The all-sky survey will be performed repeating the same basic observing mode, sketched in Figure 14. After locking the guider, a ~ 30 s broad-band image will be taken and corrected for dark, bad pixels and flat field using calibration frames stored on-board. A software routine (similar to the one we used in Sect. 6.1) will then automatically select the targets, generate and upload the optimal DMD configuration. In the mean time, the prism will be inserted at the place of the broad-band filter. We allocate 5 minutes for these operations, which will proceed in parallel on the four channels.

As mentioned in Sect. 6, refinements are possible, e.g. splitting the acquisition of spectra in multiple exposures to eliminate cosmic rays or to optimize the extraction of the bright sources. The HAWAII 2RG detectors allow to address and read individual pixels while the others integrate (guide mode). This capability may also be exploited to synchronize the readout of certain areas with the opening of the corresponding slits.

The long exposures performed for the Deep Survey will be more efficient, avoiding the frequent broad-band acquisition. We plan to add telescope dithering to recover spatial resolution and dead pixels. For the integral field spectroscopic survey of the Galactic plane, we will use Hadamard transform spectroscopy. Proposed by J. Mather for NIRSPEC on JWST and successfully
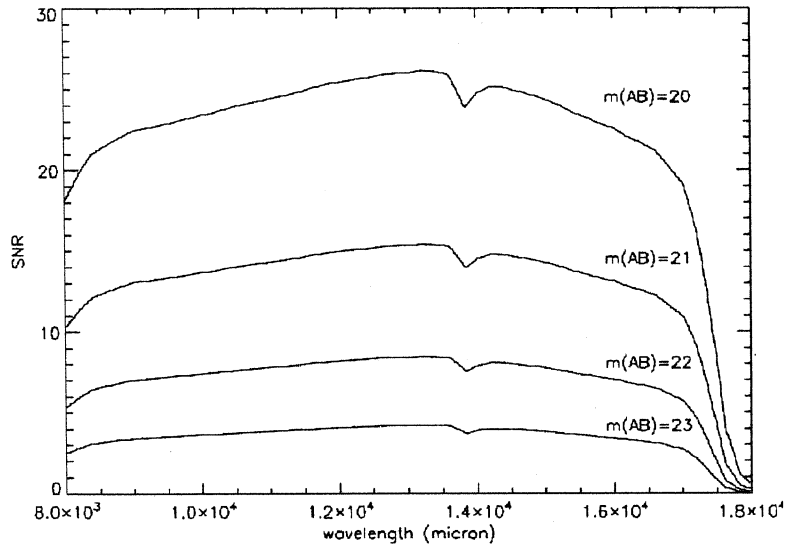
Fig. 13 Estimated SNR of SPACE spectra in 900s integration. We used detector parameters typical of WFC3/IR flight candidates. Transmission efficiencies of all reflective and refractive components are those of the WFC3/IR optical coating. Light losses due to the prism thickness are included, together with the most recent zodiacal background prediction for the SNAP mission also at L2.
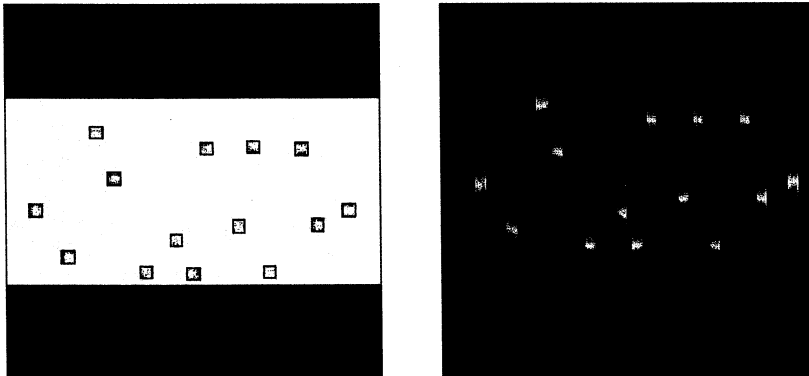
Fig. 14 Sketch of the data acquisition and observing procedure. Left: the DMD field is projected onto the detector (dark background) in broad band imaging mode. The light blue color indicates the high background, targets are represented by yellow squares. Right: all DMDs are turned off except those of the targets, the prism is inserted. The background is low (dark blue) and spectra are produced.

validated with IRMOS ([14]), this technique can be regarded as a variation of long slit spectroscopy. By opening multiple slits at the same time, over-lapped spectra are obtained. By using different slit patterns, the entire set of overlapped spectra can be eventually disentangled and the entire data cube (x, y, λ) reconstructed. Our estimates for the Galactic plane survey allocates four hours per pointing, which corresponds to individual exposures of the order of order of ~ 15 s. The lower signal to noise of the raw images will allow for a more robust compression factor than the noiseless $5\times$ used for the standard observations. The actual implementation of the Hadamard transform mode will require further analysis.

11 The *SPACE* Mission

Soyuz-Fregat is our proposed launcher. Soyuz, equipped with the Fregat up-per stage, launched from Kourou, is capable of delivering a 2-ton spacecraft directly into L2 transfer orbit without any need for large on-board propulsion. A typical duration of the transfer is 4 months. Once L2 has been reached, the delta-v requirements for orbit maintenance and formation keeping are small, a few m/s/year. The launcher provides a fairing 3.8 m wide and up to 8.5m high (with 14.5° taper above 5 m), which can easily accommodate the spacecraft configuration with an external baffle for stray light rejection.

In the survey phase, the sequence of operations is particularly simple (20 to 30 pointing, small slew, new pointing, and so on), easily automated and man-aged. Targeted observations will require similar sequences. A ground station such as Cebreros or New Norcia will have L2 above the horizon for more than 8 per day on average, with a minimum of 6 hours/day in the most unfavorable season for the given location in the Northern or Southern hemisphere. Our most conservative assumptions on compression (5 Mbit/s) and transmission (1.5 Mbit/s) require a station scheduled 3.5 hours per day for *SPACE*.

SPACE telemetry and command will be received/transmitted by a dedi-cated antenna at a single ESA Ground Station having the task of gathering the downlinked housekeeping and science telemetry and uploading the commands needed to control spacecraft and payload. The Ground Station will be shared with other missions having similar visibility requirements. The telemetry will be sent through a dedicated redundant line of appropriate bandwidth to a Mission Operations Centre (MOC) under the control of ESA. The MOC is in charge of checking the housekeeping telemetry to verify the safety of spacecraft and payload, taking if needed the appropriate corrective actions by means of commands sent following pre-specified procedures. The stream of housekeeping and science telemetry, through an ESA-provided dedicated redundant line of appropriate bandwidth, will be then ingested into a Science Operations Cen-tre (SOC) under the control of the *SPACE* Consortium. The SOC will also generate the commands needed for the satellite pointing and observations, and send them to the MOC in the form of agreed-upon procedures.

The SOC will distribute the data to a Science Data Centre (SDC), which will focus on the spectra contained in the images, their extraction, analysis, distribution, archiving and generation of scientific results. The SDC will represent the interfaces between the project and the scientific community. The SDC will receives both the raw data and pre-reduced data from the SOC, adding all services needed to efficiently exploit their science content.

The SPACEteam: Austria: W. Zeilinger (U.Wien); France: E. Daddi (CEA Saclay,), M. Lehnert, F. Hammer (Meudon), O. Le Fevre, J.-P. Kneib, J.-G. Cuby, L. Tresse, R. Grange, B. Milliard, M. Saisse (LAM); Germany: S. White, G. Kauffmann, B. Ciardi, G. De Lucia, J. Blaizot (MPA Garching), F. Bertoldi (U. Bonn), E. Schinnerer, A. Martinez-Sansigre, F. Walter, J. Kurk, J. Steinacker (MPIA Heidelberg): International: P. Rosati, P. Padovani (ESO); D. Macchetto (ESA); Italy: A. Ferrara (SISSA), A. Franceschini (U. Padova), A. Renzini (INAF OAPD), S. Cristiani, M. Magliocchetti, E. Pian, F. Pasian, A. Zacchei (INAF OATS), G. Zamorani, M. Mignoli, L. Pozzetti, C. Gruppioni, A. Comastri (INAF OABO), N. Mandolesi, R. C.Butler, C. Burigana, L. Nicastro, F. Finelli, L. Valenziano, G. Morgante, L. Stringhetti, F. Villa, F. Cuttaia, E. Palazzi, A. De Rosa, A. Gruppuso, A. Bulgarelli, F. Gianotti, M. Trifoglio, F. Paresce (INAF IASFBO), L. Guzzo, F. Zerbi, E. Molinari, P. Span (INAF Milano), R. Salvaterra (U. Milano), M. Bersanelli (U. Milano), D. Maccagni, B. Garilli, M. Scodeggio, D. Bottini, P. Franzetti (INAF IASFMI), T. Oliva (Arcetri, TNG); Netherlands: M. Franx, H. Roettgering, M. Kriek (U. Leiden); Romania: L. Popa (U. Bucharest); Spain: R. Rebolo, M. Zapatero Osorio, M. Balcells (IAC), A. Perez Garrido, A. Diaz Sanchez, I. Villo Perez (UPCT, U. Politecnica de Cartagena); Switzerland: H. Shea (cole Polytechnique Lausanne); United Kingdom: C. Frenk, C. Baugh, I. Smail, S. Cole, R. Bower, T. Shanks, M. Ward (U. Durham , Inst. Comp. Cosmology), R. Content, R. Sharples, S. Morris (U. Durham, Centre for Advanced Instrumentation), J. Silk (U. Oxford), J. Dunlop, R. McLure, M. Cirasuolo (ROE), R. Kennicutt (IoA, Cambridge), M. Jarvis (U. Hertfordshire); USA: Y. Wang (U. Oklahoma), X. Fan (U. Arizona), P. Madau (UCSC), M. Stiavelli , I. N. Reid, M. Postman, R. White, S. Casertano, S. Beckwith, J. MacKenty (STScI), J. Gardner, M. Clampin, R. Kimble (GSFC), A. Szalay, R. Wyse (JHU), A. Shapley (Princeton), N. Wright (UCLA), M. Strauss (Princeton), M. Urry (Yale), A. Burgasser (MIT), J. Rayner (Hawaii), B. Mobasher (UC Riverside), M. Di Capua (UMD), L. Hillenbrand (Caltech), M. Meyer (Steward).

References

1. Albrecht A., et al. 2006, DETF report, http://home.fnal.gov/rocky/DETF/;
2. Amendola, L., 2000, Phys.Rev. D, 62, 3511 ;
3. Angulo R., et al. 2005, MNRAS, 362, L25 ;

4. Angulo R., et al. 2007, astro-ph/0702543;
5. Blake & Glazebrook K. 2003, ApJ, 594, 665;
6. Bottini D. Et al. 2005, PASP, 117, 996;
7. Bouwens R.J., Illingworth G.D., Blakeslee J.P. Franx M., 2006, ApJ, 653, 53;
8. Bouwens R. et al. 2004, ApJ, 616, L79; Bouwens R. et al. 2004, ApJ, 624, L5;
9. Capozziello et al. 2007, arXiv0706.1146;
10. Choudhury T.R. & Ferrara A., 2006, MNRAS, 371 L55;
11. Eisenstein D. et al. 2005, ApJ, 633, 560;
12. Eisenstein D. et al. 2006, astro.ph.4362E;
13. Fan, X., et al., 2004, AJ, 128, 515;
14. Fixsen & MacKenty 2007, in prep.;
15. Guzzo L. et al. 2007, Nature, in press
16. Hamilton A.J.S. 2001, Technical Report, NASA GSFC;
17. Hu & Haiman 2003, PhRvD, 68, 6;
18. Huff E. et al. 2007, APh, 26, 351 ;
19. Hütsi G. 2005, A&A, 449, 891;
20. Hütsi G. 2006, A&A, 459, 375;
21. Kashlinsky A., 2005, PhR, 409, 361;
22. Kinney, A., Calzetti D., Bohlin R.C. et al. 1996, ApJ, 467, 38
23. Linder E., arXiv:0708.0024
24. Linder E., arXiv:0709.1113
25. Lue A., Scoccimarro R., Starkman G.D. 2004, Phys.Rev. D, 69, 124015;
26. MacKenty & Stiavelli 2000, ASP Conf. 195, 443;
27. MacKenty et al. 2006, SPIE 6269, 37M;
28. Mannucci, F., Basile F., Poggianti B. 2001, MNRAS, 326, 745
29. Martini P. & DePoy D.L., 2000, Proc. SPIE, Vol. 4008, p. 695;
30. Moseley et al. 2000, ASP Conf. 207, 262;
31. Mullis C. et al. 2005, ApJ, 623, L85;
32. Padmanabhan, T. 2007, arXiv0705.2533;
33. Peacock, J.A., et al 2006, ESA-ESO Working Group Report on Fundamental Cosmology, astro-ph/0610906;
34. Percival et al. 2007, arXiv0705.3323;
35. Perlmutter, S., et al. 1999, ApJ, 517, 565;
36. Pierleoni M. et al. 2007, submitted ;
37. Riess, A.G., et al. 1998, AJ, 116, 1009;
38. Riess, A.G., et al. 2007, ApJ, 659, 98;
39. Rosati P. et al. 2004, AJ, 127, 230;
40. Salvaterra R., Magliocchetti M., Ferrara A., Schneider R., 2006, MNRAS, 368, L6;
41. Sanchez, A.G., et al. 2006, MNRAS, 366, 189 ;
42. Scannapieco E., Schneider R., Ferrara A., 2003, ApJ, 589, 35;
43. Schaerer D., 2003, A&A, 397, 527;
44. Shapley, A., Steidel C.C., Pettini M. et al. 2003, ApJ, 588, 65
45. Seo H.-J. & D. Eisenstein 2003, ApJ, 598, 720;
46. Seo H.-J. & D. Eisenstein 2005, ApJ, 633, 575;
47. Sigad Y. et al. 2000, ApJ, 540, 62;
48. Simcoe, R.A., 2006, AJ, 653, 977;
49. Spergel et al. 2007, ApJS, 170, 377;
50. Stanford S.A. et al. 2006, ApJ, 646, L13;
51. Tegmark, M. 2003, Science, 296, 1427;
52. Tegmark et al 2006, PhRvD, 74, 12;
53. Trotta R., 2006, arXiv:astro-ph/0607496
54. Ketchum, W., and Wang, Y. 2007, submitted to ApJ (2007);
55. Venemans, B., et al., 2007, MNRAS, 376L, 76
56. Verde L. et al. 2001, MNRAS, 325, 412;
57. Vestergaard, M. 2002 ApJ, 571, 733-752
58. Wang Y. 2006, ApJ, 647, 1;
59. Wang Y. 2007, arXiv:0710.3885
60. White S.D.M., Rees M. 1978, MNRAS, 183, 341;
61. Willott, et al., 2005, ApJ, 633, 630;
62. Woods-Vasey, W.M., et al. 2007, astro-ph/0701041;